


RESEARCH ARTICLE

Left parietal involvement in motion sickness susceptibility revealed by multimodal magnetic resonance imaging

Hiroyuki Sakai¹  | Takumi Harada¹ | Stephen K. Larroque² | Athena Demertzi³ | Tomoko Sugawara¹ | Taeko Ito⁴ | Yoshiro Wada⁴ | Masaki Fukunaga⁵ | Norihiro Sadato⁵ | Steven Laureys²

¹Toyota Central R&D Laboratories, Inc., Tokyo, Japan

²Coma Science Group, GIGA-Consciousness, GIGA Institute, University of Liège, Liège, Belgium

³Physiology of Cognition Research Lab, GIGA-Consciousness, GIGA Institute, University of Liège, Liège, Belgium

⁴Department of Otolaryngology-Head and Neck Surgery, Nara Medical University, Kashihara, Japan

⁵Division of Cerebral Integration, Department of System Neuroscience, National Institute for Physiological Sciences, Okazaki, Japan

Correspondence

Hiroyuki Sakai, Toyota Central R&D Laboratories, Inc., Tokyo, 160-0004, Japan.
Email: sakai@mosk.tytlabs.co.jp

Abstract

Susceptibility to motion sickness varies greatly across individuals. However, the neural mechanisms underlying this susceptibility remain largely unclear. To address this gap, the current study aimed to identify the neural correlates of motion sickness susceptibility using multimodal MRI. First, we compared resting-state functional connectivity between healthy individuals who were highly susceptible to motion sickness ($N = 36$) and age/sex-matched controls who showed low susceptibility ($N = 36$). Seed-based analysis revealed between-group differences in functional connectivity of core vestibular regions in the left posterior Sylvian fissure. A data-driven approach using intrinsic connectivity contrast found greater network centrality of the left intraparietal sulcus in high- rather than in low-susceptible individuals. Moreover, exploratory structural connectivity analysis uncovered an association between motion sickness susceptibility and white matter integrity in the left inferior fronto-occipital fasciculus. Taken together, our data indicate left parietal involvement in motion sickness susceptibility.

KEYWORDS

conflict, motion sickness, MRI, resting state, vestibular, visual

1 | INTRODUCTION

Susceptibility to motion sickness varies greatly across individuals. A questionnaire-based survey of life-span experiences of motion sickness (Golding, 1998) indicated that some individuals have never experienced motion sickness, whereas others almost always experience motion sickness symptoms (e.g., nausea) when traveling in any type of vehicle. According to another survey that examined the prevalence of motion sickness in provocative situations (i.e., traveling on busses or ferries), a maximum of one-third of passengers reported feeling motion sickness (Lawther & Griffin, 1988; Turner & Griffin, 1999). For those who are prone to motion sickness, the value of travel is

undermined due to unpleasant symptoms, such as nausea and vomiting. Not only can they not fully benefit from freedom of movement currently, but they are even predicted to suffer from more frequent and severe motion sickness in the era of autonomous driving (Diels & Bos, 2016). To develop preventive measures for susceptible individuals, a deep understanding of the underlying pathological mechanisms is required.

Despite large individual differences in susceptibility to motion sickness, the neural mechanisms underlying these differences remain largely unclear. It is well-known that patients with bilateral vestibular loss are less likely to experience motion sickness (Paillard et al., 2013). In addition, in microgravity environments, individuals with greater

This is an open access article under the terms of the Creative Commons Attribution-NonCommercial License, which permits use, distribution and reproduction in any medium, provided the original work is properly cited and is not used for commercial purposes.

© 2021 Toyota Central R&D Labs., Inc. *Human Brain Mapping* published by Wiley Periodicals LLC.

bilateral asymmetry in otolith sensitivity are more susceptible to motion sickness than those with less asymmetry (Lackner, Graybiel, Johnson, & Money, 1987; Markham & Diamond, 1993; Sugawara, Wada, Ito, & Sakai, 2021). These lines of evidence suggest the involvement of peripheral vestibular function in motion sickness susceptibility. However, to our best knowledge, no studies have identified the neural correlates of such susceptibility in the brain.

Reciprocal interactions between visual and vestibular cortical regions may be associated with motion sickness susceptibility. One of the earliest neuroimaging studies on vestibular sensation showed that vestibular stimulation evokes activation in vestibular areas and deactivation in visual areas (Wenzel et al., 1996). It is also evident that visual stimulation evokes activation in visual areas accompanied by deactivation in vestibular areas (Brandt, Bartenstein, Janek, & Dieterich, 1998). These findings suggest the existence of reciprocal inhibitory interactions between visual and vestibular cortical regions. Some previous studies have hypothesized that such reciprocal visual-vestibular interactions may play a crucial role in resolving sensory conflicts that cause motion sickness (Brandt & Dieterich, 1999; Dieterich & Brandt, 2015). However, no empirical data have yet been provided to support this conjecture.

Recent studies have demonstrated more complex visual-vestibular interactions. It was long thought that a subregion around the posterior Sylvian fissure corresponds to a human homolog of the primate parieto-insular vestibular cortex (PIVC) (Cardin & Smith, 2010). However, Frank, Baumann, Mattingley, and Greenlee (2014); Frank, Wirth, and Greenlee (2016) revealed that the perisylvian vestibular region can be further divided into two regions that have different sensitivities to visual stimuli. One is part of the parietal operculum, referred to as the human PIVC, which is activated by vestibular stimuli and suppressed by visual stimuli. The other is the posterior insular cortex (PIC), which is activated by both vestibular and visual stimuli. A recent investigation of structural connectivity in the vestibular network (Indovina et al., 2020) demonstrated that the PIVC is more connected to sensorimotor regions, whereas the PIC is more connected to occipito-parieto-temporal regions. This suggests that the PIC, rather than the PIVC, may play a key role in visual-vestibular interactions and, therefore, motion sickness susceptibility.

The current study aimed to identify the neural correlates of motion sickness susceptibility by using functional and structural magnetic resonance imaging (MRI). First, by using both a hypothesis-driven, seed-based approach and a hypothesis-free, data-driven approach, we compared resting-state functional connectivity between healthy individuals who were highly susceptible to motion sickness and age/sex-matched controls who showed low susceptibility. For the former approach, we used each perisylvian vestibular core region (i.e., bilateral PIVC and PIC) as a seed to examine the involvement of visual-vestibular interactions in motion sickness susceptibility. For the latter, we conducted intrinsic connectivity contrast (ICC) analysis (Martuzzi et al., 2011), which can explore network centrality associated with motion sickness susceptibility on the basis of global functional connectivity, defined as the degree to which each voxel is functionally connected to the rest of the brain. Furthermore, we

performed tract-based spatial statistics (TBSS) analysis (Smith et al., 2006) to explore the structural connectivity associated with motion sickness susceptibility.

2 | MATERIALS AND METHODS

2.1 | Participants

Healthy adults aged 20–50 years were recruited via an advertisement on an employment website and paid for their participation. In all, 402 applicants completed the motion sickness susceptibility questionnaire (MSSQ) (Golding, 1998) and answered questions concerning their medical histories on the employment website. The MSSQ assesses experiences of typical motion sickness symptoms (e.g., nausea and vomiting) for each of nine types of vehicles (e.g., cars, buses, and ships) during childhood (before 12 years of age) and during the last 10 years by using a five-point Likert scale (0: never; 1: rarely; 2: sometimes; 4: frequently; and 5: always). The MSSQ score, which is calculated as the total summed symptom rating scaled by the number of vehicle types experienced, is considered a good predictor of motion sickness susceptibility during provocative motion stimulation (Golding, 2006). Figure 1a is a histogram of the MSSQ scores of all applicants. Following the questionnaire, 38 applicants with MSSQ scores >70 were voluntarily enrolled in the study; these formed the motion sickness susceptible (MSS) group (13 men and 25 women, ranging in age from 20 to 49). Age/sex-matched applicants with MSSQ scores <15 were also voluntarily enrolled in the study; these formed the motion sickness resistant (MSR) group. The cut-off points for the MSR and MSS groups were, respectively, determined on the basis of the 20th and 80th percentile scores of a healthy sample of the general population in a previous study by Golding (1998). Age was matched within 3 years on either side. According to self-reported medical histories, all participants were free of neurological or psychiatric disorders and had no history of taking psychotropic medications. Right handedness was confirmed by the Edinburgh Handedness Inventory (Oldfield, 1971). In addition, to confirm the robustness of grouping based on motion sickness susceptibility, all screened participants completed the MSSQ again on-site. Each participant provided written informed consent to participate in the study. The experimental protocols, which were approved by the ethical committees of Toyota Central R&D Laboratories, Inc. and the National Institute for Physiological Sciences, conformed to the principles of the Declaration of Helsinki.

2.2 | Assessment of vestibular function

The functional normality of vestibular end organs was ascertained via clinical examinations performed by otolaryngologists (T. I. and Y. W.). The clinical examinations comprised a structured interview, subjective visual vertical (SVV) test (Friedmann, 1970), and video head-impulse test (vHIT) (MacDougall, Weber, McGarvie, Halmagyi, & Curthoys, 2009). In the structured interview, an otolaryngologist carefully obtained histories of vestibular disorders and their potential

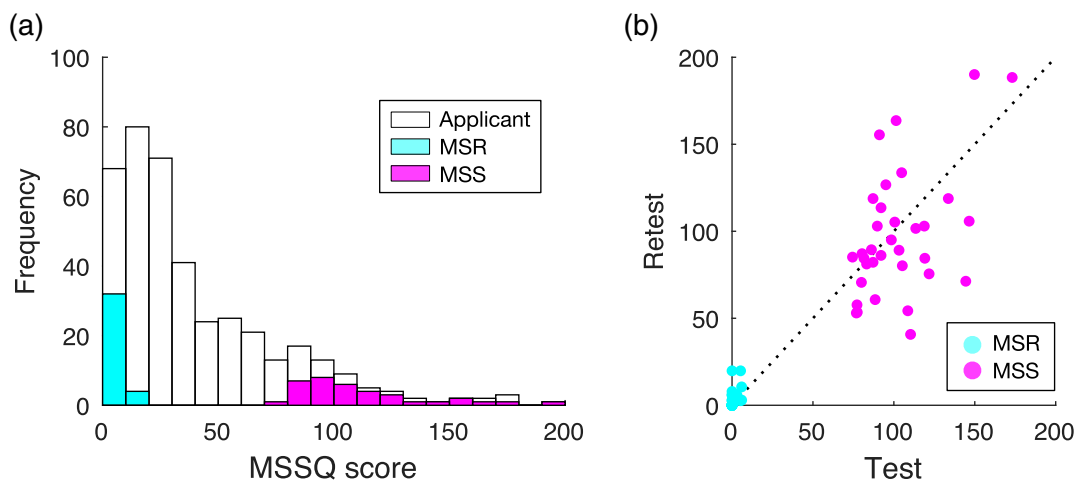


FIGURE 1 Motion sickness susceptibility in the study population. A total of 402 applicants completed the motion sickness susceptibility questionnaire (MSSQ) on the website (a). As a result of screening, 36 applicants with MSSQ scores >70 were enrolled as the motion sickness susceptible (MSS) group. Age/sex-matched applicants with MSSQ scores <15 were enrolled as the motion sickness resistant (MSR) group. MSSQ scores were measured again on-site in both the MSR and MSS groups to assess the test-retest reliability of the MSSQ (b)

symptoms, such as vertigo and dizziness. The SVV test was conducted to evaluate otolith function by using a computer-aided measurement system (UniMec, Tokyo, Japan). For the SVV test, an absolute tilt angle $> |2.5^\circ|$ was employed as a criterion for exclusion of participants (Tribukait, 2006). The vHIT, conducted by using an EyeSeeCam head-mounted video-oculography device (EyeSeeTech, Munich, Germany), enabled the assessment of semicircular canal function in response to abrupt, passive head rotations in the yaw direction. For the vHIT, a vestibulo-ocular reflex (VOR) gain (i.e., eye velocity over head velocity) <0.7 was adopted as an exclusion criterion (Yip, Glaser, Frenzel, Bayer, & Strupp, 2016). After the exclusion of participants who met these criteria and their age/sex-matched counterparts, scores for both tests were compared between the MSR and MSS groups using the Welch-corrected *t* test for unpaired data with the significance criterion set to $p < .05$. This ensured the homogeneity of both groups in terms of vestibular function.

2.3 | Data acquisition

For resting-state fMRI, functional images were acquired by using a multiband echo planar imaging (EPI) sequence on a Siemens Verio 3T MRI scanner (Siemens Medical System, Erlangen, Germany) with a 32-channel head coil. The imaging parameters were as follows: a repetition time (TR) of 750 ms, an echo time (TE) of 31 ms, a flip angle of 55, a field of view of $210 \times 210 \text{ mm}^2$, a matrix size of 100×100 , a slice thickness of 2.1 mm, 72 contiguous transverse slices, and a multiband acceleration factor of 8. A time series of 640 EPI images and a single-band reference image were collected during a scan that lasted approximately 8.2 min. During scanning, participants were instructed to fixate on a black Maltese cross on a gray background, make spontaneous eye blinks, remain awake and motionless, and not think of anything in particular. After resting-state fMRI scanning, spin echo EPI images (TR of

7,700 ms, TE of 60 ms, and flip angle of 78) were also acquired in both anterior-to-posterior and posterior-to-anterior phase encoding directions to correct for spatial distortion of the EPI images.

In addition to functional images, we acquired multiple structural images. A T1-weighted high-resolution structural image was obtained by using an MP-RAGE sequence (Mugler & Brookeman, 1990). The imaging parameters were as follows: a TR of 2,400 ms; a TE of 1.78 ms; a flip angle of 8; a field of view of $240 \times 256 \text{ mm}^2$, a matrix size of 300×320 , a slice thickness of 0.8 mm, 240 contiguous sagittal slices, and an acceleration factor of 2 for the GRAPPA parallel imaging technique (Griswold et al., 2002). Diffusion-weighted images were obtained by using a multiband EPI sequence with diffusion sensitization gradients applied in 30 noncollinear directions (*b*-value of $1,000 \text{ s/m}^2$) with one initial and three intermixed nondiffusion-weighted (*b*₀) images (*b*-value of 0 s/m^2). The imaging parameters were as follows: a TR of 3,600 ms; a TE of 85 ms; a flip angle of 78; a field of view of $198 \times 198 \text{ mm}^2$; a matrix size of 110×110 ; a slice thickness of 1.8 mm; 84 contiguous transverse slices; and a multiband acceleration factor of 3. To correct for spatial distortions, this sequence was performed twice by using anterior-to-posterior and posterior-to-anterior phase encoding directions. A high-resolution structural image of the inner ear apparatus was also obtained to examine the impact of geometrical asymmetry of the bilateral semicircular canals on motion sickness susceptibility. Full details of this image have been reported elsewhere (Harada et al., 2021).

2.4 | Functional connectivity

For each participant, the acquired EPI images, including a single-band reference image, were realigned to the last EPI image to correct for head motion using SPM12 (v7487; www.fil.ion.ucl.ac.uk/spm). Spatial distortion of the realigned EPI images was then corrected by using FSL

topup (version 5.0.8; www.fsl.fmrib.ox.ac.uk/fsl) and a pair of spin echo EPI images with opposite phase encoding directions. To obtain a deformation field for achieving accurate normalization of EPI images, the T1-weighted structural image was processed by using the CAT12 toolbox (r 1184; www.neuro.uni-jena.de/cat). After visual inspection for motion artifacts and manual realignment to the anterior commissure/posterior commissure line, the structural image was bias-corrected and segmented into gray matter, white matter and cerebrospinal fluid. Subsequently, these segmented tissue images were spatially normalized to MNI (Montreal Neurological Institute) space by using the DARTEL technique (Ashburner, 2007) and resampled with an isotropic voxel resolution of $1.5 \times 1.5 \times 1.5 \text{ mm}^3$. This process provided a deformation field for normalization. We used the default CAT12 settings with the exception of the space template for affine regularization, for which we selected the International Consortium for Brain Mapping space template for East Asian brains. Finally, the EPI images were all coregistered to the structural images via the single-band reference image, normalized by using the deformation field, and then smoothed by using an isotropic Gaussian kernel with a full width at half maximum of 8 mm.

To examine the involvement of visual-vestibular interactions in motion sickness susceptibility, we performed seed-to-voxel resting-state functional connectivity analysis by using the CONN toolbox (version 17. f; www.nitrc.org/projects/conn). First, we applied the anatomical component correction method (aCompCor) (Behzadi, Restom, Liu, & Liu, 2007) to regress out physiological noise and the ART toolbox (www.nitrc.org/projects/artifact_detect) to scrub volumes compromised by motion-related artifacts. We also applied a temporal band-pass filter, retaining signals within the frequency range of 0.008–0.09 Hz. Seed regions representing cortical vestibular processing were determined as spheres with a radius of 5 mm, according to the latest structural study (Indovina et al., 2020): $x = -36, y = -25, z = 18$ for the left PIVC; $x = 36, y = -22, z = 17$ for the right PIVC; $x = -46, y = -33, z = 24$ for the left PIC; and $x = 51, y = -27, z = 28$ for the right PIC. For each seed region, we compared functional connectivity between the two groups with a cluster-forming threshold of $p < .005$ uncorrected (two-sided) and a cluster-level threshold of $p < .05$ corrected for multiple comparisons by using family-wise error.

We also performed ICC analysis to explore functional networks associated with motion sickness susceptibility without a priori assumptions. That is, we compared global functional connectivity (i.e., ICC value) voxel-wise between the two groups. Subsequently, between-group differences in the functional connectivity of each resulting cluster was further examined by using conventional seed-to-voxel analysis (Martuzzi et al., 2011). Clusters large enough to pass a cluster-level threshold of family-wise error corrected $p < .05$ with a voxel-level threshold of $p < .005$ uncorrected (two-sided) were considered statistically significant in both the ICC and follow-up analyses.

2.5 | Structural connectivity

We performed TBSS analysis using FSL to explore white matter integrity associated with motion sickness susceptibility. For each

participant, the pair of diffusion-weighted images acquired with opposite phase encoding directions was converted into a fractional anisotropy (FA) map with a preprocessing procedure implemented in MRtrix3 (<http://www.mrtrix.org>). This procedure included denoising, eddy correction, and tensor fitting. Individual FA maps were registered to the FMRIB58-FA template in MNI space and averaged to produce a mean FA map. The mean FA map was thinned and thresholded at $FA > 0.2$ to generate a study-specific FA skeleton, representing the centers of tracts common to all participants. Then, all of the individual FA maps were projected onto the skeleton and compared voxel-wise between the groups. The criterion for statistical significance was set to $p < .05$, with the threshold-free cluster enhancement corrected for multiple comparisons by using 5,000 permutations (Smith & Nichols, 2009).

3 | RESULTS

3.1 | Group characteristics

As a result of screening, two female participants in the MSS group (aged 20 and 39 years) met the exclusion criteria for vestibular functioning. These two and their matched participants in the MSR group were excluded from further analysis. Although there was a significant difference in MSSQ scores between the MSR and MSS groups ($t(35.3) = 21.5, p < .001$) (Figure 1a), we found no significant between-group differences in vestibular functioning (Table 1): absolute tilt angles assessed via the SVV test ($t(69.9) = 1.09, p = .28$); VOR gains assessed via the vHIT (for leftward head rotation, $t(65.7) = 0.93, p = .36$; for rightward head rotation, $t(69.8) = 0.23, p = .82$).

In addition, we examined the test-retest reliability of the MSSQ to ensure the robustness of grouping based on motion sickness susceptibility (Figure 1b). The overall correlation between test and retest MSSQ scores across all screened participants was very high ($r = .92, p < .001$). In contrast, within-group correlations were significant but moderate (MSR: $r = .48, p = .003$; MSS: $r = .66, p < .001$). These

TABLE 1 Group characteristics

	MSR	MSS	<i>p</i>
<i>n</i> (male/female)	13/23	13/23	–
Age	26.9 (8.9)	26.9 (9.5)	–
MSSQ score	0.9 (1.9)	106.9 (29.5)	< .001
SVV score	1.20 (0.74)	1.00 (0.78)	.28
vHIT gain, left	1.06 (0.14)	1.02 (0.18)	.36
vHIT gain, right	1.11 (0.18)	1.12 (0.19)	.82

Note: MSS and MSR represent motions sickness susceptible and resistant groups, respectively. Figures are means and SDs (in parentheses) except for the number of participants, *n*. *p* denotes *p*-values for between-group comparisons using the Welch-corrected *t* test for unpaired data. Abbreviations: MSR, motion sickness resistant; MSS, motion sickness susceptible; SVV, subjective visual vertical; vHIT, video head-impulse test.

results suggest that, although the order of individual susceptibility scores within each group could vary across tests, the grouping of the MSR and MSS groups was robust and reliable.

3.2 | Functional connectivity

We found variations in the functional network among vestibular seed regions. Comparisons of functional connectivity between the ipsilateral PIVC and PIC across all participants (regardless of motion sickness susceptibility) revealed that the PIVC was more functionally connected to the sensorimotor cortex, including the paracentral lobule; in contrast, the PIC was more connected to the temporoparietal region covering the supramarginal gyrus and the posterior superior temporal gyrus (Figure S1). These differences are comparable to the results achieved by a structural vestibular network investigation (Indovina et al., 2020).

Regarding between-group comparisons of vestibular networks, significant differences were found in the functional connectivity of left vestibular seed regions. The left PIC seed showed greater negative connectivity with the medial occipital cortex, including the calcarine sulcus ($x = -2$, $y = -74$, $z = 2$; $k = 406$), in the MSR group than in the MSS group (Figure 2a). The left PIVC seed showed greater negative connectivity with the left superior frontal gyrus (SFG; $x = 18$, $y = 20$, $z = 46$; $k = 270$) in the MSS group than in the MSR group (Figure 2b). There were no significant differences in the functional connectivity of right vestibular seed regions.

The ICC analysis revealed a significant cluster in the left posterior intraparietal sulcus (IPS; $x = -26$, $y = -62$, $z = 42$; $k = 257$). This cluster exhibited significantly greater network centrality (global functional connectivity) in the MSS group than in the MSR group (Figure 3). In fact, a follow-up seed-to-voxel analysis using the significant cluster showed stronger (both positive and negative) functional connectivity over extensive cortical areas in the MSS group than in the MSR group (Figure S2). However, none of the clusters reached statistical significance after correction for multiple comparisons. This suggests that the greater network centrality of the left posterior IPS cluster in the MSS group is not attributable to a region-specific increase in functional connectivity.

3.3 | Structural connectivity

The TBSS analysis revealed a significant cluster with higher FA values in the MSS group than in the MSR group in the posterior part of the left inferior fronto-occipital fasciculus (IFOF; $x = -30$, $y = -70$, $z = 1$; $k = 243$) (Figure 4). The opposite contrast (i.e., MSS < MSR) uncovered no significant clusters.

4 | DISCUSSION

The neural mechanisms underlying individual variation in motion sickness susceptibility remain unclear. To address this issue, this study aimed to identify neural correlates of motion sickness susceptibility

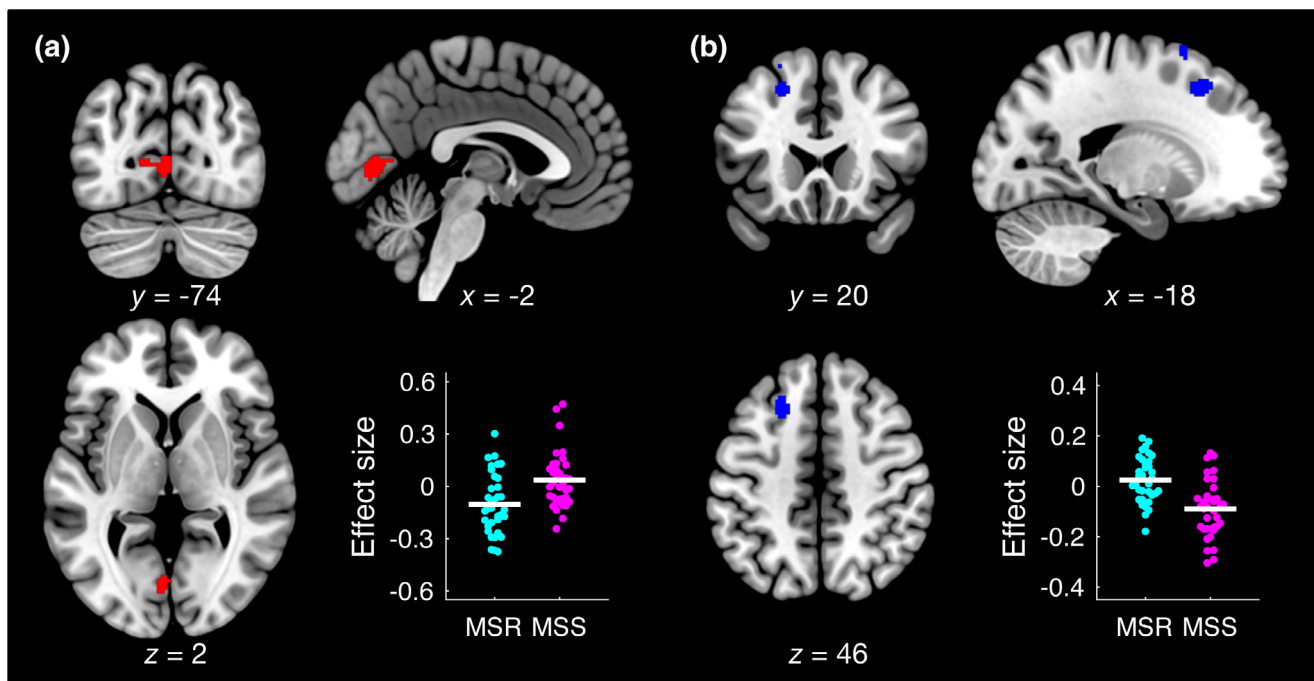


FIGURE 2 Functional vestibular network involved in motion sickness susceptibility. The left posterior insular cortex showed greater negative connectivity with the medial occipital cortex, including the calcarine sulcus ($x = -2$, $y = -74$, $z = 2$; $k = 406$), in the motion sickness resistant (MSR) group than in the motion sickness susceptible (MSS) group (a). The left parieto-insular vestibular cortex showed greater negative connectivity with the left superior frontal gyrus ($x = -18$, $y = 20$, $z = 46$; $k = 270$) in the MSS group than in the MSR group (b)

by using multimodal MRI. Our data demonstrated that functional and structural variations in networks centered on the left parietal cortex were associated with motion sickness susceptibility, although there is evidence of right hemisphere dominance for vestibular processing (Dieterich et al., 2003).

The current seed-to-voxel analysis revealed that functional connectivity between the left PIC and the medial occipital cortex was

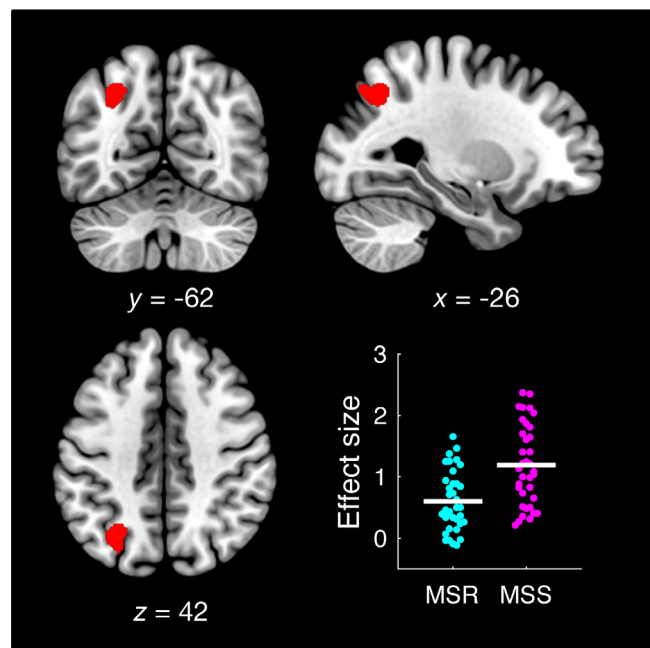


FIGURE 3 Regional network centrality associated with motion sickness susceptibility. The left posterior intraparietal sulcus (IPS; $x = -26$, $y = -62$, $z = 42$; $k = 257$) showed greater network centrality (global functional connectivity) in the motion sickness resistant (MSR) group than in the motion sickness susceptible (MSS) group. This cluster was used as a seed region in the follow-up seed-to-voxel functional connectivity analysis

associated with motion sickness susceptibility. Greater negative functional connectivity of the vestibular core region with the primary visual area in the MSR group seems consistent with the view in the literature (Brandt & Dieterich, 1999; Dieterich & Brandt, 2015) that reciprocal visual-vestibular interactions may play a role in resolving sensory conflicts that cause motion sickness. In addition, the attenuated negative functional connectivity between vestibular and visual areas in the MSS group is consistent with a previous positron emission tomography study demonstrating the co-activation of vestibular and visual areas in a situation of sensory conflict between vestibular and visual inputs (Deutschländer et al., 2002). Although the interpretation of negative functional connectivity is still under debate (Murphy, Birn, Handwerker, Jones, & Bandettini, 2009), these findings constitute the first empirical evidence that reciprocal visual-vestibular interactions are associated with motion sickness susceptibility.

The seed-to-voxel analysis also revealed an association between motion sickness susceptibility and functional connectivity between the left PIVC and the left SFG. A meta-analysis of neuroimaging studies using vestibular stimuli revealed that a left SFG region in the vicinity of the frontal eye field is activated during caloric vestibular stimulation (Lopez, Blanke, & Mast, 2012). This is consistent with the notion that vestibular responses in the frontal lobe play some role in controlling the VOR (Fukushima, Akao, Kurkin, Kaneko, & Fukushima, 2006). However, the SFG cluster observed in our study is far anterior to the frontal eye field (Paus, 1996). Regenbogen et al. (2017) showed that a similar region in the SFG was activated by sensory sickness cues (e.g., face color) in other individuals. Such a sensitivity of the SFG to sensory sickness cues may underlie its functional connectivity with the vestibular cortex in individuals susceptible to motion sickness, although vestibular signals convey sensory sickness cues for the self rather than for others.

Moreover, the current analysis revealed greater network centrality in the left posterior IPS in the MSS group than in the MSR group. Several lines of evidence have implicated the IPS in vestibular processing. Suzuki et al. (2001) showed that the IPS is activated bilaterally, despite

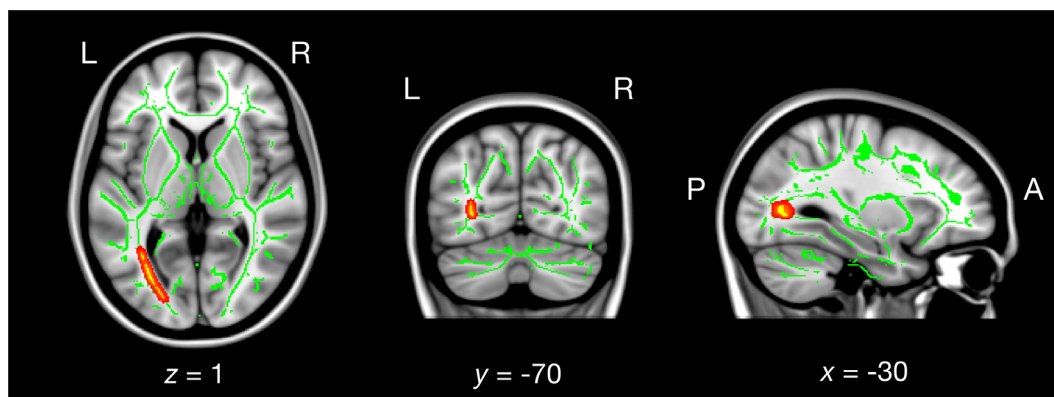


FIGURE 4 White matter integrity associated with motion sickness susceptibility. The posterior part of the left inferior fronto-occipital fasciculus ($x = -30$, $y = -70$, $z = 1$; $k = 243$) showed higher white matter integrity in the motion sickness susceptible (MSS) group than in the motion sickness resistant (MSR) group. The significant cluster is thickened for purposes of visualization (yellow-red) and overlaid on the mean skeleton (green). L, R, A, and P denote left, right, anterior, and posterior, respectively

the presence of right dominance, by caloric stimulation of the vestibular organ. Miyamoto, Fukushima, Takada, de Waele, and Vidal (2007) also reported bilateral IPS activation in response to vestibular stimulation via loud clicks. In addition, a previous transcranial direct current stimulation (tDCS) study by Arshad et al. (2014) showed that the application of tDCS over the parietal region bilaterally could modulate the VOR. Given that vestibular sensation is critical to the pathogenesis of motion sickness (Paillard et al., 2013), our results seem to be consistent with these previous findings that the IPS plays a role in vestibular processing. However, the IPS is not dedicated solely to vestibular processing but is also implicated in various sensory and cognitive functions, including visual processing (Swisher, Halko, Merabet, McMains, & Somers, 2007), auditory processing (Foster & Zatorre, 2010), tactile processing (Bodegård, Geyer, Grefkes, Zilles, & Roland, 2001), spatial 244 attention (Gillebert et al., 2011), and numerical processing (Ashkenazi, Henik, Ifergane, & Shelef, 2008). Therefore, the current data do not rule out the possibility that more complicated functional aspects of the IPS mediate motion sickness susceptibility; rather, they suggest that the left posterior IPS may act as a functional hub that integrates multisensory information, including vestibular signals, and is therefore a critical substrate for motion sickness susceptibility.

The involvement of the left posterior IPS in motion sickness susceptibility provides new insights into therapeutic interventions. In fact, a tDCS study by Arshad et al. (2015) has already demonstrated that application of cathodal inhibitory stimulation over the left parietal cortex results in increased tolerance to motion sickness during exposure to a provocative motion stimulus. The participants also experienced reduced recovery time from motion sickness after removal of the motion stimulation. In addition, exploring therapeutic motion-sickness interventions based on the multifunctionality of the IPS may prove to be a fruitful and novel avenue for future research. For example, given the involvement of the IPS in numerical processing (Ashkenazi et al., 2008) and the evidence for an interaction between vestibular and numerical processing (Arshad, Nigmatullina, Nigmatullin, et al., 2016; Arshad, Nigmatullina, Roberts, et al., 2016; Ferrè, Day, Bottini, & Haggard, 2013; Moser, Vibert, Caversaccio, & Mast, 2017), future studies may reveal that motion sickness susceptibility can be changed by performing certain numerical tasks.

The present findings represent the first evidence linking higher white matter integrity (i.e., a higher FA value) with motion sickness susceptibility. Although it is well established that the left IFOF plays an important role in semantic processing (Duffau, 2008; Duffau et al., 2005), little is known about its roles in sensory processing. However, an anatomical dissection study by Martino, Brogna, Robles, Vergani, and Duffau (2010) indicated that the IFOF connects the frontal lobe (including the insula) not only with the occipital gyrus but also with the parietal lobe, suggesting that it contributes to the integration of multimodal sensory information. The higher white matter integrity in the left IFOF may underlie functional connectivity changes in the left hemisphere in individuals susceptible to motion sickness. Future investigation should begin to reveal the functional roles of the IFOF in motion sickness susceptibility.

Taken together, our findings seem to suggest that there may be left hemispheric dominance for motion sickness susceptibility. This appears to be consistent with previous work, which demonstrated the preventive effects of perturbations to the left parietal cortex on motion sickness (Arshad et al., 2015). However, the functional and structural alterations in the left hemisphere that we found in the present study do not necessarily indicate left hemispheric dominance. To conclude that there is left hemispheric dominance for motion sickness susceptibility, in addition to identifying the areas involved, we need a comprehensive understanding of the neural networks that include such areas, including any interhemispheric inhibition (Arshad, Nigmatullina, Nigmatullin, et al., 2016). Although left hemisphere dominance for motion sickness susceptibility is an interesting hypothesis, we must wait for future studies to provide further evidence to reach similar conclusions as those in the examples of language and spatial neglect.

Our findings should be interpreted with consideration of several limitations. First, this was a cross-sectional study. Therefore, the neural correlates that we observed could have been consequences, rather than causes, of motion sickness susceptibility. For example, frequent experiences of nausea during motion sickness might cause neural plastic changes in sensory and visceral networks. Second, the frequency and variation of vehicle use are potential confounding factors that could account for the differences between the two experimental groups. Recent studies have suggested that experiences of vehicle use can modify brain structures (Maguire et al., 2000; Megías et al., 2018; 280 Sakai, Ando, Sadato, & Uchiyama, 2017) and functions (Wang, Liu, Shen, Li, & Hu, 2015). Third, motion sickness susceptibility was, retrospectively, and comprehensively assessed by using a questionnaire. A more direct evaluation of motion sickness susceptibility in specific provocative conditions may establish more specific information regarding the underlying neural mechanisms.

5 | CONCLUSION

Motion sickness is an unsolved problem with a long history that impedes freedom of movement, and it is expected to become even more serious with the spreading of self-driving cars (Diels & Bos, 2016). To develop preventive measures, we need a deeper understanding of its underlying mechanisms. In the current study, we found that motion sickness susceptibility was associated with functional and structural networks centered on the left parietal cortex. Future research should explore, on the basis of the underlying neural mechanisms, therapeutic interventions for individuals who are susceptible to motion sickness. Hypothesis-free data-driven approaches, such as ICC analysis, may be particularly beneficial in uncovering unexpected intervention points.

CONFLICT OF INTERESTS

H. S., T. H., and T. S. were employed by Toyota Central R&D Laboratories, Inc. The remaining authors declare that the research was

conducted in the absence of any commercial or financial relationships that could be construed as a potential conflict of interest.

DATA AVAILABILITY STATEMENT

The data that support the findings of this study are available from the corresponding author upon reasonable request.

ORCID

Hiroyuki Sakai  <https://orcid.org/0000-0001-8928-6591>

REFERENCES

- Arshad, Q., Cerchiai, N., Goga, U., Nigmatullina, Y., Roberts, R. E., Casani, A. P., ... Bronstein, A. M. (2015). Electroconvulsive therapy for motion sickness. *Neurology*, *85*, 1257–1259.
- Arshad, Q., Nigmatullina, Y., Nigmatullin, R., Asavarut, P., Goga, U., Khan, S., ... Malhotra, P. A. (2016). Bidirectional modulation of numerical magnitude. *Cerebral Cortex*, *26*, 2311–2324.
- Arshad, Q., Nigmatullina, Y., Roberts, R. E., Bhurugubanda, V., Asavarut, P., & Bronstein, A. M. (2014). Left cathodal transcranial direct current stimulation of the parietal cortex leads to an asymmetrical modulation of the vestibular-ocular reflex. *Brain Stimulation*, *7*, 85–91.
- Arshad, Q., Nigmatullina, Y., Roberts, R. E., Goga, U., Pikovsky, M., Khan, S., ... Bronstein, A. M. (2016). Perceived state of self during motion can differentially modulate numerical magnitude allocation. *European Journal of Neuroscience*, *44*, 2369–2374.
- Ashburner, J. (2007). A fast diffeomorphic image registration algorithm. *NeuroImage*, *38*, 95–113.
- Ashkenazi, S., Henik, A., Ifergane, G., & Shelef, I. (2008). Basic numerical processing in left intraparietal sulcus (IPS) acalculia. *Cortex*, *44*, 439–448.
- Behzadi, Y., Restom, K., Liu, J., & Liu, T. T. (2007). A component based noise correction method (CompCor) for BOLD and perfusion based fMRI. *NeuroImage*, *37*, 90–101.
- Bodegård, A., Geyer, S., Grefkes, C., Zilles, K., & Roland, P. E. (2001). Hierarchical processing of tactile shape in the human brain. *Neuron*, *31*, 317–328.
- Brandt, T., Bartenstein, P., Janek, A., & Dieterich, M. (1998). Reciprocal inhibitory visual-vestibular interaction. Visual motion stimulation deactivates the parieto-insular vestibular cortex. *Brain*, *121*, 1749–1758.
- Brandt, T., & Dieterich, M. (1999). The vestibular cortex. Its locations, functions, and disorders. *Annals of the New York Academy of Sciences*, *871*, 293–312.
- Cardin, V., & Smith, A. T. (2010). Sensitivity of human visual and vestibular cortical regions to egomotion-compatible visual stimulation. *Cerebral Cortex*, *20*, 1964–1973.
- Deuschländer, A., Bense, S., Stephan, T., Schwaiger, M., Brandt, T., & Dieterich, M. (2002). Sensory system interactions during simultaneous vestibular and visual stimulation in PET. *Human Brain Mapping*, *16*, 92–103.
- Diels, C., & Bos, J. E. (2016). Self-driving carsickness. *Applied Ergonomics*, *53*(Pt B), 374–382.
- Dieterich, M., Bense, S., Lutz, S., Drzegza, A., Stephan, T., Bartenstein, P., & Brandt, T. (2003). Dominance for vestibular cortical function in the non-dominant hemisphere. *Cerebral Cortex*, *13*, 994–1007.
- Dieterich, M., & Brandt, T. (2015). The bilateral central vestibular system: Its pathways, functions, and disorders. *Annals of the New York Academy of Sciences*, *1343*, 10–26.
- Duffau, H. (2008). The anatomo-functional connectivity of language revisited. New insights provided by electrostimulation and tractography. *Neuropsychologia*, *46*, 927–934.
- Duffau, H., Gatignol, P., Mandonnet, E., Peruzzi, P., Tzourio-Mazoyer, N., & Capelle, L. (2005). New insights into the anatomo functional connectivity of the semantic system: A study using cortico-subcortical electrostimulations. *Brain*, *128*, 797–810.
- Ferrè, E. R., Day, B. L., Bottini, G., & Haggard, P. (2013). How the vestibular system interacts with somatosensory perception: A sham-controlled study with galvanic vestibular stimulation. *Neuroscience Letters*, *550*, 35–40.
- Foster, N. E. V., & Zatorre, R. J. (2010). A role for the intraparietal sulcus in transforming musical pitch information. *Cerebral Cortex*, *20*, 1350–1359.
- Frank, S. M., Baumann, O., Mattingley, J. B., & Greenlee, M. W. (2014). Vestibular and visual responses in human posterior insular cortex. *Journal of Neurophysiology*, *112*, 2481–2491.
- Frank, S. M., Wirth, A. M., & Greenlee, M. W. (2016). Visual-vestibular processing in the human Sylvian fissure. *Journal of Neurophysiology*, *116*, 263–271.
- Friedmann, G. (1970). The judgement of the visual vertical and horizontal with peripheral and central vestibular lesions. *Brain*, *93*, 313–328.
- Fukushima, J., Akao, T., Kurkin, S., Kaneko, C. R. S., & Fukushima, K. (2006). The vestibular-related frontal cortex and its role in smooth-pursuit eye movements and vestibular-pursuit interactions. *Journal of Vestibular Research*, *16*, 1–22.
- Gillebert, C. R., Mantini, D., Thijs, V., Sunaert, S., Dupont, P., & Vandenberghe, R. (2011). Lesion evidence for the critical role of the intraparietal sulcus in spatial attention. *Brain*, *134*, 1694–1709.
- Golding, J. F. (1998). Motion sickness susceptibility questionnaire revised and its relationship to other forms of sickness. *Brain Research Bulletin*, *47*, 507–516.
- Golding, J. F. (2006). Predicting individual differences in motion sickness susceptibility by questionnaire. *Personality and Individual Differences*, *41*, 237–248.
- Griswold, M. A., Jakob, P. M., Heidemann, R. M., Nittka, M., Jellus, V., Wang, J., ... Haase, A. (2002). Generalized autocalibrating partially parallel acquisitions (GRAPPA). *Magnetic Resonance in Medicine*, *47*, 1202–1210.
- Harada, T., Sugawara, T., Ito, T., Wada, Y., Fukunaga, M., Sadato, N., ... Sakai, H. (2021). Vestibular morphological asymmetry associated with motion sickness susceptibility. *Frontiers in Neuroscience*, *15*, 763040. <https://doi.org/10.3389/fnins.2021.763040>
- Indovina, I., Bosco, G., Riccelli, R., Maffei, V., Lacquaniti, F., Passamonti, L., & Toschi, N. (2020). Structural connectome and connectivity lateralization of the multimodal vestibular cortical network. *NeuroImage*, *222*, 117247.
- Lackner, J. R., Graybiel, A., Johnson, W. H., & Money, K. E. (1987). Asymmetric otolith function and increased susceptibility to motion sickness during exposure to variations in gravito-inertial acceleration level. *Aviation, Space, and Environmental Medicine*, *58*, 652–657.
- Lawther, A., & Griffin, M. J. (1988). A survey of the occurrence of motion sickness amongst passengers at sea. *Aviation, Space, and Environmental Medicine*, *59*, 399–406.
- Lopez, C., Blanke, O., & Mast, F. W. (2012). The human vestibular cortex revealed by coordinate-based activation likelihood estimation meta-analysis. *Neuroscience*, *212*, 159–179.
- MacDougall, H. G., Weber, K. P., McGarvie, L. A., Halmagyi, G. M., & Curthoys, I. S. (2009). The video head impulse test: Diagnostic accuracy in peripheral vestibulopathy. *Neurology*, *73*, 1134–1141.
- Maguire, E. A., Gadian, D. G., Johnsrude, I. S., Good, C. D., Ashburner, J., Frackowiak, R. S., & Frith, C. D. (2000). Navigation related structural change in the hippocampi of taxi drivers. *Proceedings of the National Academy of Sciences of the United States of America*, *97*, 4398–4403.
- Markham, C. H., & Diamond, S. G. (1993). A predictive test for space motion sickness. *Journal of Vestibular Research*, *3*, 289–295.

- Martino, J., Brogna, C., Robles, S. G., Vergani, F., & Duffau, H. (2010). Anatomic dissection of the inferior fronto-occipital fasciculus revisited in the lights of brain stimulation data. *Cortex*, *46*, 691–699.
- Martuzzi, R., Ramani, R., Qiu, M., Shen, X., Papademetris, X., & Constable, R. T. (2011). A whole-brain voxel based measure of intrinsic connectivity contrast reveals local changes in tissue connectivity with anesthetic without a priori assumptions on thresholds or regions of interest. *NeuroImage*, *58*, 1044–1050.
- Megjás, A., Petrova, D., Navas, J. F., Cándido, A., Maldonado, A., & Catena, A. (2018). Neuroanatomical variations as a function of experience in a complex daily task: A VBM and DTI study on driving experience. *Brain Imaging and Behavior*, *12*, 653–662.
- Miyamoto, T., Fukushima, K., Takada, T., de Waele, C., & Vidal, P. P. (2007). Saccular stimulation of the human cortex: A functional magnetic resonance imaging study. *Neuroscience Letters*, *423*, 68–72.
- Moser, I., Vibert, D., Caversaccio, M. D., & Mast, F. W. (2017). Acute peripheral vestibular deficit increases redundancy in random number generation. *Experimental Brain Research*, *235*, 627–637.
- Mugler, J. P., & Brookeman, J. R. (1990). Three-dimensional magnetization-prepared rapid gradient-echo imaging (3D MP RAGE). *Magnetic Resonance in Medicine*, *15*, 152–157.
- Murphy, K., Birn, R. M., Handwerker, D. A., Jones, T. B., & Bandettini, P. A. (2009). The impact of global signal regression on resting state correlations: Are anti-correlated networks introduced? *NeuroImage*, *44*, 893–905.
- Oldfield, R. C. (1971). The assessment and analysis of handedness: The Edinburgh inventory. *Neuropsychologia*, *9*, 97–113.
- Paillard, A. C., Quarck, G., Paolino, F., Denise, P., Paolino, M., Golding, J. F., & Ghulyan-Bedikian, V. (2013). Motion sickness susceptibility in healthy subjects and vestibular patients: Effects of gender, age and trait-anxiety. *Journal of Vestibular Research*, *23*, 203–209.
- Paus, T. (1996). Location and function of the human frontal eye-field: A selective review. *Neuropsychologia*, *34*, 475–483.
- Regenbogen, C., Axelsson, J., Lasselin, J., Porada, D. K., Sundelin, T., Peter, M. G., ... Olsson, M. J. (2017). Behavioral and neural correlates to multisensory detection of sick humans. *Proceedings of the National Academy of Sciences of the United States of America*, *114*, 6400–6405.
- Sakai, H., Ando, T., Sadato, N., & Uchiyama, Y. (2017). Greater cerebellar gray matter volume in car drivers: An exploratory voxel-based morphometry study. *Scientific Reports*, *7*, 46526.
- Smith, S. M., Jenkinson, M., Johansen-Berg, H., Rueckert, D., Nichols, T. E., Mackay, C. E., ... Behrens, T. E. J. (2006). Tract-based spatial statistics: Voxelwise analysis of multi-subject diffusion data. *NeuroImage*, *31*, 1487–1505.
- Smith, S. M., & Nichols, T. E. (2009). Threshold-free cluster enhancement: Addressing problems of smoothing, threshold dependence and localisation in cluster inference. *NeuroImage*, *44*, 83–98.
- Sugawara, T., Wada, Y., Ito, T., & Sakai, H. (2021). Bilateral asymmetry in ocular counter-rolling reflex is associated with individual motion sickness susceptibility. *Frontiers in Neurology*, *12*, 759764. <https://doi.org/10.3389/fneur.2021.759764>
- Suzuki, M., Kitano, H., Ito, R., Kitanishi, T., Yazawa, Y., Ogawa, T., ... Kitajima, K. (2001). Cortical and subcortical vestibular response to caloric stimulation detected by functional magnetic resonance imaging. *Cognitive Brain Research*, *12*, 441–449.
- Swisher, J. D., Halko, M. A., Merabet, L. B., McMains, S. A., & Somers, D. C. (2007). Visual topography of human intraparietal sulcus. *The Journal of Neuroscience*, *27*, 5326–5337.
- Tribukait, A. (2006). Subjective visual horizontal in the upright posture and asymmetry in roll-tilt perception: Independent measures of vestibular function. *Journal of Vestibular Research*, *16*, 35–43.
- Turner, M., & Griffin, M. J. (1999). Motion sickness in public road transport: Passenger behavior and susceptibility. *Ergonomics*, *42*, 444–461.
- Wang, L., Liu, Q., Shen, H., Li, H., & Hu, D. (2015). Large-scale functional brain network changes in taxi drivers: Evidence from resting-state fMRI. *Human Brain Mapping*, *36*, 862–871.
- Wenzel, R., Bartenstein, P., Dieterich, M., Danek, A., Weindl, A., Minoshima, S., ... Brandt, T. (1996). Deactivation of human visual cortex during involuntary ocular oscillations. A PET activation study. *Brain*, *119*, 101–110.
- Yip, C. W., Glaser, M., Frenzel, C., Bayer, O., & Strupp, M. (2016). Comparison of the bedside head-impulse test with the video head-impulse test in a clinical practice setting: A prospective study of 500 outpatients. *Frontiers in Neurology*, *7*, 58.

SUPPORTING INFORMATION

Additional supporting information may be found in the online version of the article at the publisher's website.

How to cite this article: Sakai, H., Harada, T., Larroque, S. K., Demertzi, A., Sugawara, T., Ito, T., Wada, Y., Fukunaga, M., Sadato, N., & Laureys, S. (2022). Left parietal involvement in motion sickness susceptibility revealed by multimodal magnetic resonance imaging. *Human Brain Mapping*, *43*(3), 1103–1111. <https://doi.org/10.1002/hbm.25710>